Applied Surface Science 421 (2017) 748–754

Contents lists available at ScienceDirect

Applied Surface Science

journal homepage: www.elsevier.com/locate/apsusc

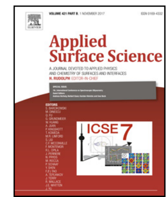

Full Length Article

Spectroscopic ellipsometry and X-ray diffraction studies on $Si_{1-x}Ge_x$/Si epifilms and superlattices

Deng Xie [a,b], Zhi Ren Qiu [b,*], Lingyu Wan [c], Devki N. Talwar [d], Hung-Hsiang Cheng [e], Shiyuan Liu [f], Ting Mei [g], Zhe Chuan Feng [c]

[a] Institute of Optoelectronic Material and Technology, South China Normal University, 510631 Guangzhou, China
[b] State Key Laboratory of Optoelectronic Materials and Technologies and School of Physics, Sun Yat-Sen University, 510275 Guangzhou, China
[c] Laboratory of optoelectronic materials & detection technology, Guangxi Key Laboratory for the Relativistic Astrophysics, College of Physics Science & Technology, Guangxi University, 530004 Nanning, China
[d] Department of Physics, Indiana University of Pennsylvania,975 Oakland Avenue, 56 Weyandt Hall, IN, PA 15705-1087, USA
[e] Center for Condensed Matter Sciences and Graduate Institute of Electronics Engineering, National Taiwan University, Taipei 106, Taiwan
[f] State Key Laboratory of Digital Manufacturing Equipment and Technology, Huazhong University of Science and Technology, 430074 Wuhan, China
[g] The Key Laboratory of Space Applied Physics and Chemistry, Ministry of Education and Shaanxi Key Laboratory of Optical Information Technology, School of Science, Northwestern Polytechnical University, 710072 Xi'an, China

ARTICLE INFO

Article history:
Received 31 July 2016
Received in revised form 2 February 2017
Accepted 6 March 2017
Available online 8 March 2017

Keywords:
Spectroscopic ellipsometry
X-ray diffraction
Silicon germanium

ABSTRACT

Comprehensive optical and structural properties are reported on several MBE grown thin $Si_{1-x}Ge_x$ epifilms and $Si_{1-x}Ge_x$/Si superlattices with low Ge contents by using spectroscopic ellipsometry (SE), high resolution x-ray diffraction (HR-XRD) and Raman scattering (RS). For thin $Si_{1-x}Ge_x$ films, our appraised results of the optical dielectric functions from SE spectra fitted to the parameterized models have revealed discrepancies with the existing data. While E_1 and $E_1 + \Delta_1$ critical point energies have shown similarities, their amplitudes uncovered ~25% larger value for the E_1 band-edge, and ~10% larger value for the $E_1 + \Delta_1$ band-edge. In our samples, the observed vibrational peaks in the RS are classified as unstrained Si—Si, Ge—Ge and Ge—Si modes. These mode assignments in $Si_{1-x}Ge_x$ alloys are evaluated compared and discussed with the available RS data.

© 2017 Elsevier B.V. All rights reserved.

1. Introduction

The strained $Si_{1-x}Ge_x$ epifilms and wrinkled hetero-structures grown on Si substrate received considerable attention for applications in the field of opto-electronics – especially for fabricating high speed heterojunction bipolar transistors (HBTs) [1], high-electron mobility transistors (HEMTs) and metal-oxide-semiconductor field effect transistors (MOSFETs) [2–4]. More recently, Si/$Si_{1-x}Ge_x$/Si hetero-structure materials have drawn significant interest due to their potential use for applications in advanced micro and nano electronics where complementary-metal-oxide-semiconductor (CMOS) based compatible electronic and photonic components can be integrated at lower cost and higher efficiency on Si platform. In order to realize such applications, however, a good control on the complex thin layered hetero-structure is required in terms of its film thickness and alloy composition. While, the spectroscopic ellipsometry (SE) has long been recognized as a powerful method for the non-destructive characterization of thin films and multilayer structures – several other experimental methods are attempted to characterize $Si_{1-x}Ge_x$/Si hetero-structures with *in situ* and *ex situ* configurations. In this context, the mechanical, electrical and optical properties have been explored for ultrathin $Si_{1-x}Ge_x$ material samples prepared under various growth conditions [5–14]. While limited investigations are known for assessing the optical properties – the use of different experimental tools for characterizing both optical and structural behavior of ultrathin $Si_{1-x}Ge_x$ epilayers and hetero-structures are rather sparse.

By combining several non-destructive experimental methods including SE, x-ray diffraction (XRD) and Raman scattering (RS), we have reported the results of our comprehensive investigations for appraising both structural and optical properties of different Si/$Si_{1-x}Ge_x$/Si hetero-structure material samples with small Ge contents. While the SE results of dielectric functions for each layer helped us assess thickness, surface configuration and mixture states – the analyses of XRD measurements are found extremely

* Corresponding author.
E-mail addresses: stsqzr@mail.sysu.edu.cn (Z.R. Qiu), fengzc@gxu.edu.cn (Z.C. Feng).

http://dx.doi.org/10.1016/j.apsusc.2017.03.066
0169-4332/© 2017 Elsevier B.V. All rights reserved.

Table 1
MBE growth conditions used to prepare $Si_{1-x}Ge_x$/Si(001) heterostructures.

Sample number	Structure	Temperature	Flow ratio
SG168	Superlattice (×10)	550 °C	Si:1.2 Ge:0.2
SG171	Single layer	700 °C	Si: 1 Ge: 0.1
SG203	Superlattice (×10)	700 °C	Si:3 Ge:2
SG216	Single layer	800 °C	Si: 4 Ge: 2.5
SG217	Superlattice (×10)	750 °C	Si: 4 Ge: 4

beneficial for precisely estimating layer thickness and Ge composition in all material samples. We strongly believe that the results reported here for the technologically important structures would enable us develop advanced Si-based devices on new core concepts which were recognized earlier in the field of compound semiconductors only.

2. Experimental

2.1. Molecular beam epitaxial growth

The molecular beam epitaxy (MBE) is a non-equilibrium process used for growing crystalline semiconductors via deposition of one or more types of atoms from effusion furnace or similar sources onto an existing crystalline surface under ultra-high vacuum conditions. The non-intentionally doped hetero-epitaxial $Si_{1-x}Ge_x$ samples used in the present study were grown on (001) Si substrates by using MBE system (Riber SIVA-32RD) [15] in an ultrahigh vacuum chamber with a base pressure of 5×10^{-10} Torr. A 1000 nm thick Si buffer layer deposited prior to the $Si_{1-x}Ge_x$ strained-layer growth to attain a flatter surface on Si (001) substrate. The Ge composition x in the $Si_{1-x}Ge_x$ layers was varied from 0.029 to 0.074. We kept the layer thickness growth less than 240 nm to fall well within the critical thickness derived from the force balance theory of Matthews. We set different flow ratio of Si and Ge to achieve a diverse composition of Ge in $Si_{1-x}Ge_x$ layers with growth temperature varied from 550 °C to 800 °C. Details of the growth conditions used for preparing $Si_{1-x}Ge_x$/Si(001) hetero-structures are reported in Table 1.

2.2. Spectroscopic ellipsometry

Spectroscopic ellipsometry is a non-destructive optical method for characterizing both thin and thick layers of either amorphous or crystalline material. This technique is well suited for measuring films with thicknesses of a few angstroms up to several microns, particularly for those materials that have well established values for the indices of refraction. The SE is capable of using electromagnetic wavelengths from an extreme ultra-violet to the far infrared.

The variable angle spectroscopic ellipsometry (VASE) uses change in the state of polarization of light upon reflection for *in-situ* and real-time characterization of surfaces, interfaces, and thin films. The analysis of VASE experiment in hetero-structured $Si_{1-x}Ge_x$/Si(001) multilayer system has enabled us to assess the critical point energies as well as information on thickness, crystallinity, roughness and composition of individual layers. In such experiments the measured ratio ρ of the reflection coefficient r_p and r_s can be expressed in terms of the amplitude ratio tan ψ and the phase angle Δ:

$$\rho = \left(\frac{r_p}{r_s}\right) = \left(\tan\psi\right) e^{(i\Delta)}, \quad (1)$$

where the two ellipsometry parameters ψ and Δ can be obtained directly from the SE measurements; r_p and r_s represents parallel and perpendicular reflection coefficients to the plane of incidence, respectively.

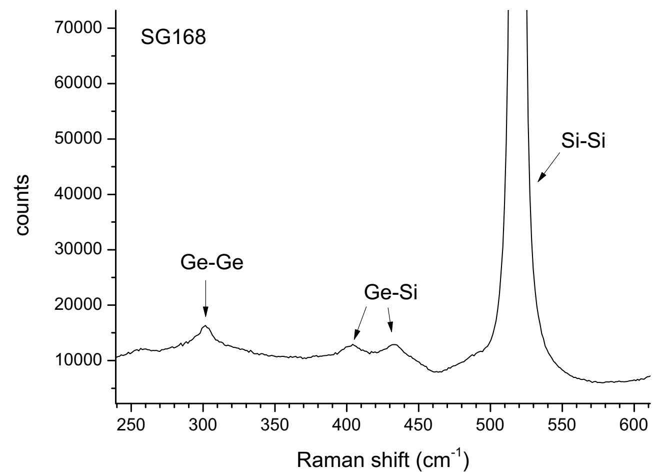

Fig. 1. 514 nm excited Raman spectra of sample SG168. Ge-Ge mode near ~302 cm^{-1} and Ge-Si mode at 404 cm^{-1} and 432 cm^{-1} are clearly denoted.

The complex dielectric function $\varepsilon(\omega)\{=\varepsilon_1(\omega)+i\varepsilon_2(\omega)\}$ can be derived from SE data by using a two-phase model:

$$\varepsilon(\omega) = \{\sin^2\Phi + \sin^2\Phi\tan^2\Phi[(1-\rho)/(1+\rho)]^2\}, \quad (2)$$

where Φ is the angle of incidence. For each sample, we carried out the SE measurements (cf. Sec. 3) for energy (wavelength) ranging between 0.73 eV (191 nm) and 6.5 eV (1690 nm) with a step size of 1.5 nm at several angle of incidence $\Phi(\equiv 60^\circ, 65^\circ$ and $70^\circ)$. The choice of different Φ ' smade here was to increase the sensitivity of the ellipsometry angles and reduce the uncertainties of the sample structure parameters (cf. Sec. 3).

2.3. X-ray diffraction

For comprehending the macroscopic strain relaxation in $Si_{1-x}Ge_x$ layers grown on Si (001) substrate, the measurements of x-ray rocking curves played an important role. In this regard the plots of intensity as a function of angle [i.e., omega – 2 theta (ω – 2θ) scans] were recorded by using the conventional high resolution "Bruker D8 advance x-ray diffractometer". The Cu Kα radiation emerging from the point focus (0.1 mm x 0.1 mm) of a rotating anode source operating at 50 kV and 20 mA was converted into a quasi-parallel beam by a parabolically graded multilayer mirror. In all $Si_{1-x}Ge_x$ samples the strain state was probed by x-ray coplanar diffraction (cf. Sec. 3) in the vicinity of the Si (004) Bragg peak.

2.4. Raman scattering

Raman scattering is a powerful technique for the characterization of semiconductors. It is non-destructive and requires no special preparation of samples. Furthermore, the Raman efficiency of this material is high because of the strong covalence of the bonding and the Raman signals are easily obtained. The Raman parameters such as intensity, width, peak frequency and polarization of Raman bands provide fruitful information on the crystal quality and material properties.

Raman scattering spectra for each $Si_{1-x}Ge_x$/Si(001) heterostructure sample was recorded having different Ge composition using an excited wavelength of 514 nm with a Renishaw confocal Raman-PL spectrometer. All RS measurements (cf. Sec. 3) in the backscattering geometry were executed at room temperature.

Table 2
Parameters values obtained by fitting the SE spectra of five different samples. In column 2, the first line represents the total layer thickness, the second line represents layer thickness of SiGe/Si in SL with 10 repeat times.

Sample No.	Total SiGe SL thickness (nm) with individual SiGe/Si layers (nm)	Si capping layer thickness (nm)	SiO_2 layer thickness (nm)	Ge content.[b]
SG168	217.83 11.13/10.65 × 10[a]	198.9	2.66	0.057
SG171	211.31	186.95	2.41	0.045
SG203	127.34 4.38/8.35 × 10[a]	72.77	2.55	0.047
SG216	14.33	55.03	2.58	0.029
SG217	239.20 15.42/8.50 × 10[a]	60.95	2.28	0.074

[a] Parameters set by XRD fitting result.
[b] Ge content is obtained by using the model (see: Ref. [20]).

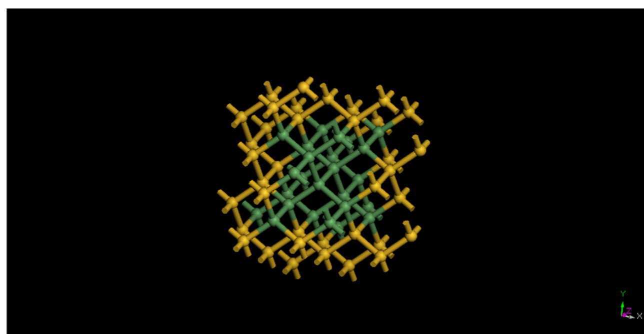

Fig. 2. Diagram of Ge cluster formed in Si bulk material. Ge atoms are colored green and Si atoms are colored orange. (For interpretation of the references to color in this figure legend, the reader is referred to the web version of this article.)

3. Results and discussion

In Fig. 1 we have displayed the results of our 514 nm excited first-order Raman spectra (FORS) for one of the $Si_{1-x}Ge_x$/Si(001) hetero-structures (SG 168). Very similar Raman line shapes (not shown here) are revealed in most other material samples. While the high frequency peak observed near ~520 cm^{-1} is designated as the Si—Si vibrational mode (cf. Fig. 1) – originating from Si-cap layer, the peak near 302 cm^{-1} is labeled as Ge-Ge mode and the other features around ~404 cm^{-1} and ~435 cm^{-1} are assigned as Si-Ge modes. One must note that a precise determination of Si-Ge and Ge-Ge mode frequencies in $Si_{1-x}Ge_x$/Si(001) are somewhat convoluted by Ge-composition induced artefacts. It is frequently suggested that Ge-composition x, may trigger weak subsidiary features in the vicinity of major FORS lines and cause asymmetric broadening in the Raman modes. The observed distorted features of both intensity and frequency in the FORS reported in the literature [16,17] include *a*) the composition dependent Ge-Ge like phonon modes appearing between ~280 cm^{-1} to ~305 cm^{-1} for x ~0.3 and *b*) Si-Ge like modes emerging in the range between ~380–512 cm^{-1} for $x > 0.3$. In our $Si_{1-x}Ge_x$/Si(001) hetero-structures with $x \leq 0.074$, we argue, however, that the appearance of Ge-Ge mode near ~302 cm^{-1} in the FORS is caused by the formation of Ge-Ge cluster in unstrained $Si_{1-x}Ge_x$ layers whereas Ge-Si bond is formed at the side of Ge clusters as shown in Fig. 2.

The results of SE measurement performed on SG 168 sample are shown in Fig. 3. The data displayed for Ψ and Δ spectra represent the amplitude and phase of the elliptical polarized light received by the detector. The SE results for other samples (not shown here) are quite similar to Fig. 3–except that some details are noticed in the interference regions. In our analyses we have considered a Si capping layer, a thick (>1000 nm) Si buffer layer and Si substrate assumed to have the same dielectric functions. We

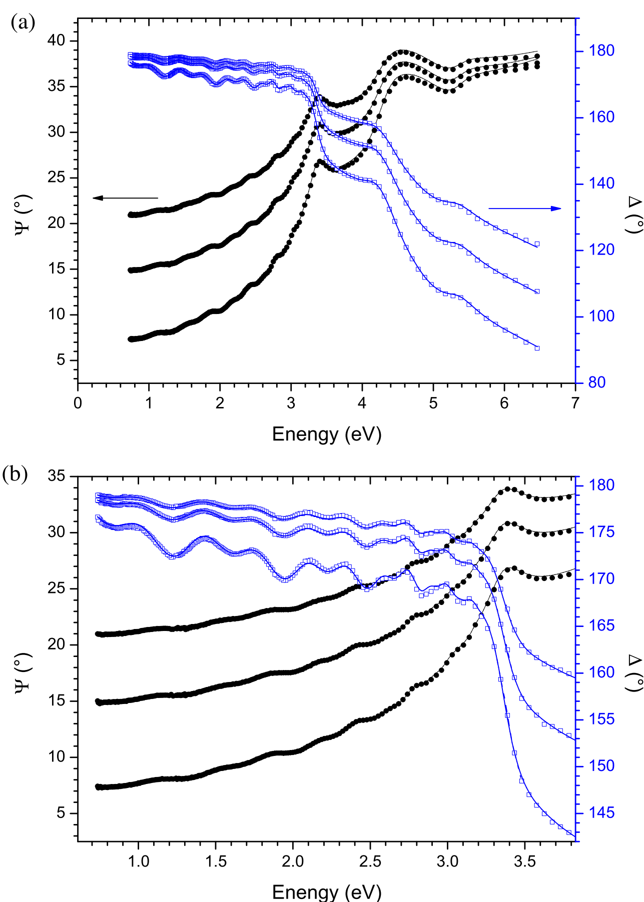

Fig. 3. (a) SE spectra and fitting result of sample SG168. (b) An exaggerated plot to show interference oscillations under band gap region. Black solid circle denotes Ψ, blue hollow square denotes Δ in experiment, and lines are fitting result. The SE results for other samples (not shown here) are quite similar to SG168. (For interpretation of the references to color in this figure legend, the reader is referred to the web version of this article.)

have also considered a SiO_2 layer above the Si capping layer, due to exposure of the sample to the air. Accordingly for assessing the optical properties of the material samples we have constructed a model having four components (e.g., SiO_2/Si/$Si_{1-x}Ge_x$/Si). Eometric software was used to simulate and fit the thickness of each layer and Ge-composition x. For the superlattice (SL) structure, we have considered thickness and composition of each repeat layer to be identical for retaining a minimum number of parameters in the fitting procedure. This choice avoids correlation between the parameters and the characteristics of SE spectra to guarantee unique values of each constraint.

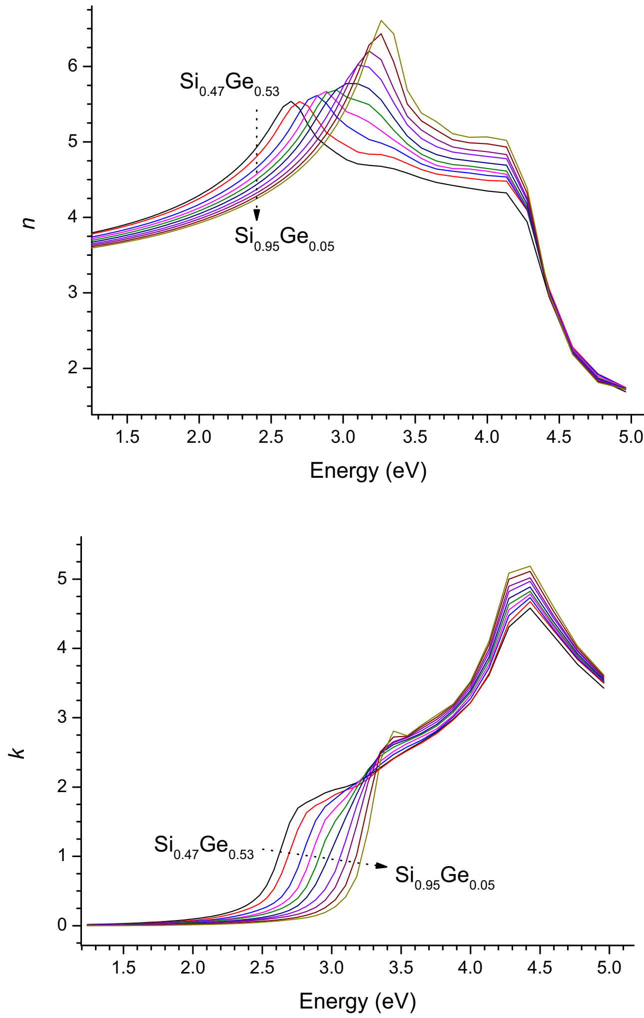

Fig. 4. Dielectric function used to simulate SiGe series in SE fitting, achieved from Ref. [20].

Many researchers have studied the composition dependent dielectric function of SiGe alloys [6,18–21]. By using a theoretical model developed by J. A. Woollam Co., we simulated here the dielectric functions (Fig. 4) of $Si_{1-x}Ge_x$ hetero-structure materials (relaxed) with the fitted parameter values from Ref. [20]. For distinct interference oscillations below the band edge around 3 eV – the best fit results with a mean square error (MSE) lower than 3.5 are obtained for all samples. The parameter values used in the fitting process for all $Si_{1-x}Ge_x$/Si(001) hetero-structure samples are reported in Table 2.

The accuracy of experimental results with model calculations is judged by using MSE, where:

$$MSE = \frac{1}{2N-M}\sum_{i=1}^{N}\left[\left(\frac{\Psi_i^{mod}-\Psi_i^{exp}}{\sigma_{\Psi,i}^{exp}}\right)^2+\left(\frac{\Delta_i^{mod}-\Delta_i^{exp}}{\sigma_{\Delta,i}^{exp}}\right)^2\right] = \frac{1}{2N-M}\chi^2. \quad (3)$$

In Eq. (3) the term N stands for the total number of experimental results of Ψ and Δ for each chosen wavelength; M represents the number of fitting parameters used; the superscripts *mod* and *exp* represent the appropriate values of model and experimental data; σ signifies the MSE between the calculated and experiment data at each wavelength while the summations over i are performed for the whole spectral range with χ being the standard deviation.

From the XRD measurements of ω-2θ, the multi-layer thickness and alloy composition was deduced from the lattice constant calculation and interference oscillation simulation – synthesized by X'pert Epitaxy software. The same multi-film structure considered in SE fitting procedure was used to fit the XRD results as well. While the main line at 34.564° is the unstrained Si (100) diffraction peak (see: Fig. 5) – the SiGe line appears, however, at the lower side of the angle due to larger atom size of Ge. Samples with SL structures show clear satellite lines except for the zero level peak. All the observed XRD features compare favorably well with the fitting results displayed in Fig. 5 with parameter values listed in Table 3. Although, we noticed strong parameter correlation with the thickness of Si and SiGe in the SL structures – there appear, however, discrepancies in the individual layer thickness while the total thickness of SL region is in good agreement.

The parameter sensitivity is also noticed in the fitting procedures of the SE spectra. From SE measurements while the thickness of the two SiGe/Si layers in the SL structure are correlated well – the entire thickness of SL region and Si capping layer exhibit unique values. On the contrary, the thickness of each layer in SL are strongly dependent on the position of satellite peaks in XRD spectra, while the Si capping layer thickness is influenced by the interference oscillation between satellite peaks, which are usually blurred and indistinct due to measurement conditions.

In Table 3 we have compared values of the Ge composition in $Si_{1-x}Ge_x$ alloys derived from SE and XRD methods. Despite some uncertainties in the Ge contents from two different methods – the results clearly show a similar trend for all samples with relatively lower values from the SE fitting procedure. According to the above discussions, we contended that dielectric function of SiGe with small Ge content could be different from the bulk materials studied in Ref. [18–20]. Concerning the Raman spectra which showed identical phonon-mode results in all samples with major peaks identified as pure unstrained Si-Si, Ge-Ge and Ge-Si modes – we argue that Ge clusters are formed in Si materials instead of a uniform mixing of these two (Si, Ge) elements.

By using a parameterized model we have simulated the dielectric function of SiGe films and deduced the E_1 and $E_1+\Delta_1$ edges and amplitudes. Two Tauc-Lorentz line shape with the following form:

$$\varepsilon_2(E)\begin{cases} = \dfrac{AE_0C(E-Eg)^2}{\left(E^2-{E_0}^2\right)^2+C^2E^2}\times\dfrac{1}{E},\ E>Eg, \\ = 0,\ E\le Eg. \end{cases} \quad (4)$$

are used to simulate E_1 and $E_1+\Delta_1$ edges, while another two Lorentz line shapes with formalism of

$$\varepsilon(E) = \frac{AB_rE_0}{E_0-E-i\cdot EB_r}, \quad (5)$$

are considered to fit the band-tail and higher energy transition, respectively. In Eq. (5) the term A stands for amplitude of the Lorentz shape absorption peak, B_r is the broadening and E_o is the position of the peak. In Tauc-Lorentz model, the real part of the dielectric function ε_1 is obtained by exploiting the Kramers–Kronig integrations i.e.,

$$\varepsilon_1(E) = \varepsilon_1(\infty)+\frac{2}{\pi}P\int_{Eg}^{\infty}\frac{\xi\varepsilon_2(\xi)}{\xi^2-E^2}d\xi. \quad (6)$$

The term P stands for the Cauchy principal part of the integral, and $\varepsilon_1(\infty)$ representing the ε value in the infrared limit is added as a fitting parameter.

The values of A and E_0 used for samples in the present study and in Refs. [18–20] are shown in Fig. 6 for comparison. The trend of E_1 and $E_1+\Delta_1$ edge with Ge content in the two series – our dilute $Si_{1-x}Ge_x$ alloys and bulk $Si_{1-x}Ge_x$ using interpolation method to define the dielectric function of dilute Ge region are identical,

Table 3
Parameters obtained by SE fitting of the five samples. In column 2, the first line represents the layer thickness as a whole, and the second line represents the layer thickness of SiGe and Si in SL region, with 10 repeat times. Ge content in column 5 is used for comparison.

Sample No.	SiGe (Si/SiGe) layer thickness (nm)	Si capping layer thickness (nm)	Ge content by XRD	Ge content by SE
SG168	217.83 11.13/10.65 × 10	196.00	0.157	0.057
SG171	210.20	203.15	0.183	0.045
SG203	127.34 4.38/8.35 × 10	72.77[a]	0.173	0.047
SG216	14.75	56.03	0.114	0.029
SG217	242.67 15.12/9.15 × 10	60.95[a]	0.217	0.074

[a] Parameters set by SE fitting result.

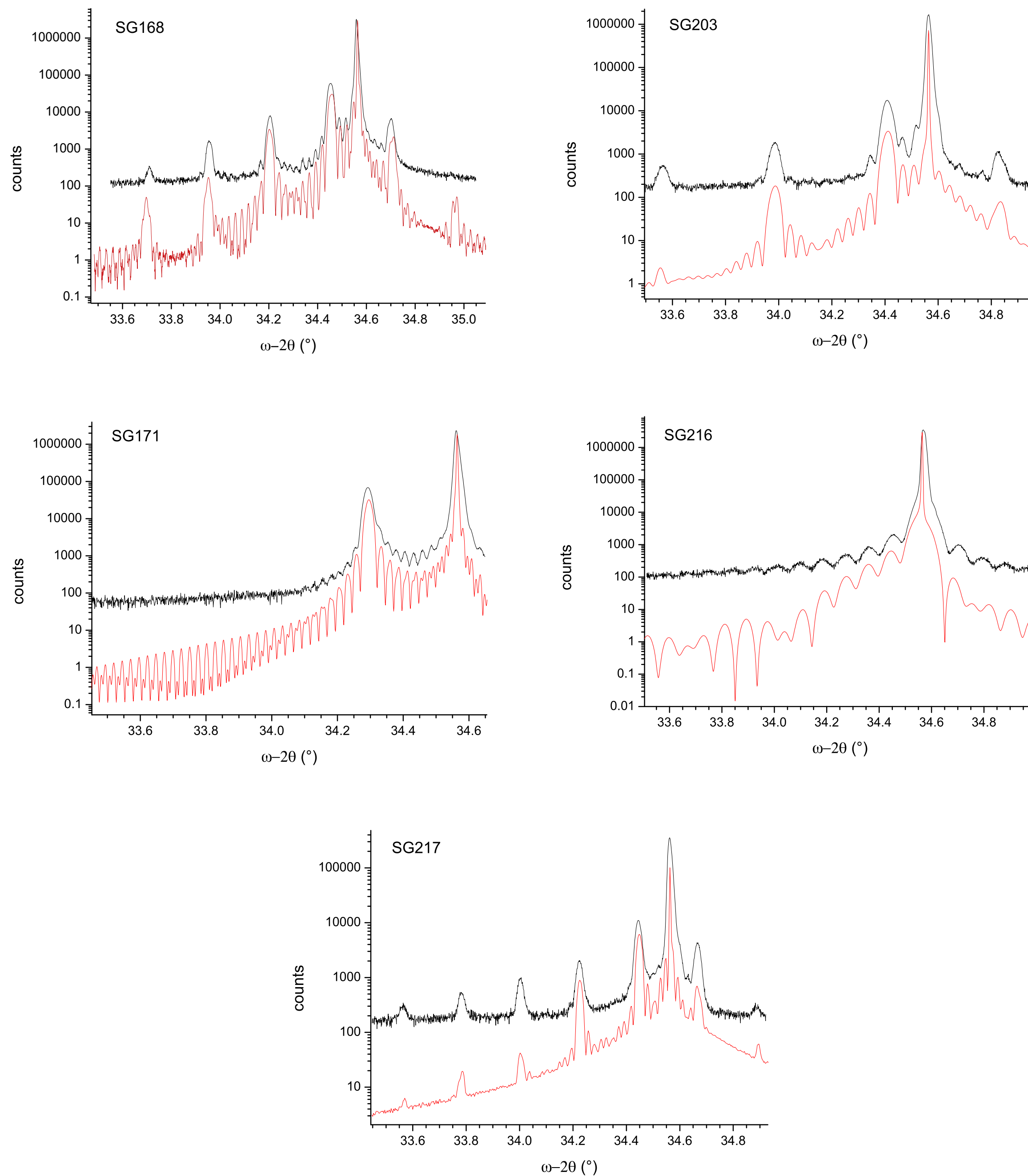

Fig. 5. XRD ω-2θ scan spectra and the fitting result by X'pert Epitaxy, with tolerance of 10^{-5}. The thickness of each layer in SL are strongly dependent on the position of satellite peaks in XRD spectra, which is the most important character to be considered in the fitting procedure.

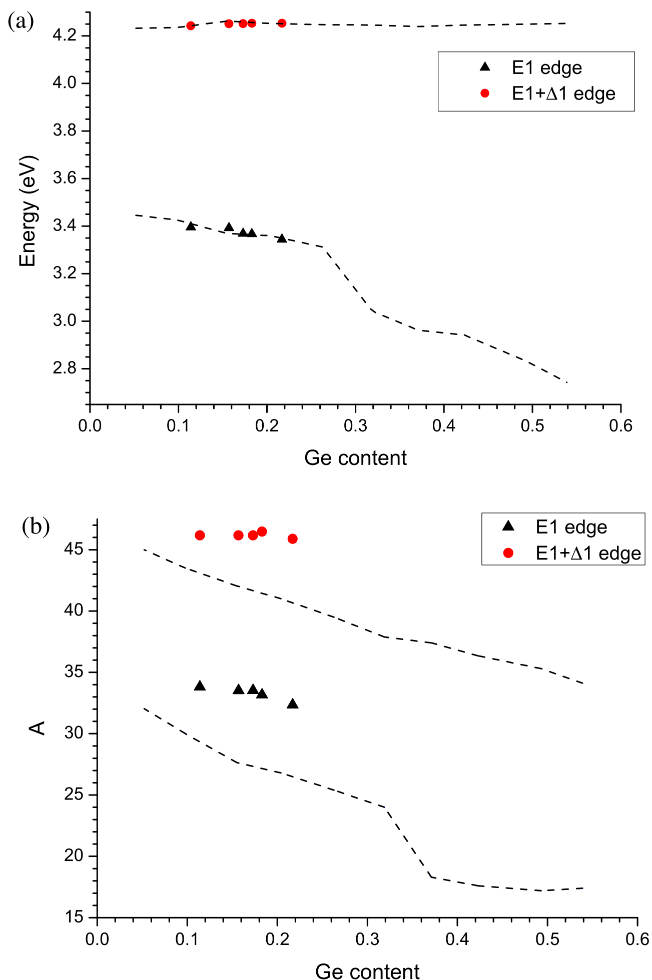

Fig. 6. The values of A and E_0 used for samples in the present study and in Refs. [18–20]. The amplitude of Si-Ge series show ~25% larger value of E_1 edge, and ~10% larger value of $E_1 + \Delta_1$ edge than reported in the literature. (a): The Ge content dependent E1 (black) and E1 + Δ1 (red) edge; (b) Amplitude of Tauc-Lorentz model at the edge. Dotted line is fitted from Ref. [20]. (For interpretation of the references to color in this figure legend, the reader is referred to the web version of this article.)

however the amplitude of Si-Ge series show ~25% larger value of E_1 edge, and ~10% larger value of $E_1 + \Delta_1$ edge than reported in the literature. This phenomenon can be regarded as the impact of Ge cluster formation in Si main material for small x.

4. Conclusion

In conclusion, we have reported the results of our comprehensive investigations by using non-destructive characterization methods to assess the optical and structural properties of $Si_{1-x}Ge_x$ thin films and $Si_{1-x}Ge_x$/Si SLs with low Ge contents. The VASE method with three different incidence angles along with high resolution XRD experiments are used here to evaluate thickness of each layer as well as Ge composition in SiGe films and SiGe/Si SLs. Due to the sensitivity of various fitting parameters – we find the combination of SE and XRD methods to be useful in analyzing the optical spectra. While the assessed values of Ge contents by SE and XRD methods are found different the results clearly showed, however, similar trends. By using parameterized models to fit the SE data, we also noticed some discrepancies in the optical dielectric functions when compared with the existing results for SiGe films. While the E_1 and $E_1 + \Delta_1$ critical point energies are identical, their amplitudes have shown ~25% larger values for the E_1 edge, and ~10% larger value for the $E_1 + \Delta_1$ edge. In all our samples, the Raman scattering spectra showed identical vibrational peaks – classified as pure unstrained Si-Si, Ge-Ge and Ge-Si modes. For the Ge-Ge mode at low Ge contents, we have argued the possibility of the formation of Ge clusters rather than a uniform mixing of Si, Ge elements in $Si_{1-x}Ge_x$ alloys as suggested in the literature [18–20]. Average t-matrix Green's function (ATM-GF) calculation based on a realistic lattice dynamical approach is underway to evaluate the observed impurity-mode behavior in dilute $Si_{1-x}Ge_x$ alloys [22].

Acknowledgements

We acknowledge the funding supports from the Open-Project Program of the State Key Laboratory of Optoelectronic Materials and Technologies (Sun Yatsen Unversity) #2012-KF-ZD4 and the National Natural Science Foundation of China under Grant Nos. 11474365, 61377055, and 61176085, and the Department of Education of Guangdong Province, China (grant no. gjhz1103). The work at Guangxi University is supported by National Natural Science Foundation of China (No. 61367004), and Guangxi Key Laboratory for the Relativistic Astrophysics-Guangxi Natural Science Creative Team funding (No. 2013GXNSFFA019001). One of us DNT acknowledges receiving "research innovation grant" from the Graduate school at Indiana University of Pennsylvania and thank Dr. Deanne Snavely for providing him the travel funds that made this collaborative research possible.

References

[1] I.Z. Mitrovic, O. Buiu, S. Hall, J. Zhang, Y. Wang, P.L.F. Hemment, H.A.W. El Mubarek, P. Ashburn, Electrical and materials characterization of GSMBE grown $Si_{1-x-y}Ge_xC_y$ layers for heterojunction bipolar transistor applications, Semicond. Sci. Technol. 20 (2005) 95–102.
[2] G.-E. Chang, C.-O. Chang, H.H. Cheng, Strain analysis of a wrinkled SiGe bilayer thin film, J. Appl. Phys. 111 (2012).
[3] A.I. Fedorchenko, H.H. Cheng, A. Koroleva, W. Wei-Chih, Wrinkled SiGe Nanofilms as a Source of Terahertz Radiation, 2014.
[4] H. Li, T.P. Chen, C. Chang, H.H. Cheng, G.-E. Chang, K.M. Hung, Diode-like electrical characteristics of SiGe wrinkled heterostructure operating under both forward and reverse bias, Appl. Phys. Lett. 108 (2016).
[5] M. Dominguez, P. Rosales, A. Torres, F. Flores, J. Molina, M. Moreno, J. Luna, A. Orduna, Effects of germane flow rate in electrical properties of a-SiGe:H films for ambipolar thin-film transistors, Thin Solid Films 562 (2014) 260–263.
[6] I.-S. Park, Y.C. Jung, J. Ahn, T.-H. Shim, D.-Y. Lee, J.-G. Park, Dielectric function of $Si_{1-x}Ge_x$ films grown on silicon-on-insulator substrates, J. Appl. Phys. 115 (2014).
[7] M. Mederos, S.N.M. Mestanza, I. Doi, J.A. Diniz, Effects of temperature and deposition time on the structural and optical properties of $Si_{1-x}Ge_x$ nanoparticles grown by low pressure chemical vapor deposition, Thin Solid Films 579 (2015) 116–122.
[8] J. Hart, R. Hazbun, D. Eldridge, R. Hickey, N. Fernando, T. Adam, S. Zollner, J. Kolodzey, Tetrasilane and digermane for the ultra-high vacuum chemical vapor deposition of SiGe alloys, Thin Solid Films 604 (2016) 23–27.
[9] R. Hazbun, J. Hart, R. Hickey, A. Ghosh, N. Fernando, S. Zollner, T.N. Adam, J. Kolodzey, Silicon epitaxy using tetrasilane at low temperatures in ultra-high vacuum chemical vapor deposition, J. Cryst. Growth 444 (2016) 21–27.
[10] K. Tao, J.-I. Hanna, Epitaxial growth of germanium-rich silicon–germanium films on Si(0 0 1) substrate by reactive thermal chemical vapor deposition, Appl. Surf. Sci. 282 (2013) 472–477.
[11] C.-Y. Chou, G.S. Hwang, On the origin of anisotropic lithiation in crystalline silicon over germanium: a first principles study, Appl. Surf. Sci. 323 (2014) 78–81.
[12] T.K.S. Wong, Y. Gong, P. Yang, C.M. Ng, Characterization of biaxial stressed silicon by spectroscopic ellipsometry and synchrotron x-ray scattering, Semicond. Sci. Technol. 22 (2007) 1232–1239.
[13] W.S. Tan, H.H. Cheng, V.I. Mashanov, Y.F. Wong, C.T. Chia, Strain modulation of SiGe virtual substrate, Appl. Phys. Lett. 88 (2006).
[14] G. Raja Muthinti, M. Medikonda, T. Adam, A. Reznicek, A.C. Diebold, Effects of stress on the dielectric function of strained pseudomorphic $Si_{1-x}Ge_x$ alloys from 0 to 75% Ge grown on Si (001), J. Appl. Phys. 112 (2012) 053519.
[15] S.W. Lee, H.C. Chen, L.J. Chen, Y.H. Peng, C.H. Kuan, H.H. Cheng, Effects of low-temperature Si buffer layer thickness on the growth of SiGe by molecular beam epitaxy, J. Appl. Phys. 92 (2002) 6880–6885.
[16] O. Pagès, J. Souhabi, V.J.B. Torres, A.V. Postnikov, K.C. Rustagi, Re-examination of the SiGe Raman spectra: percolation/one-dimensional-cluster scheme andab initiocalculations, Phys. Rev. B 86 (2012).

[17] T.R. Yang, M.M. Dvoynenko, Z.C. Feng, H.H. Cheng, Raman spectroscopy of self-assembled Ge islands on Si, Eur. Phys. J. B: Condens. Matter 31 (2003) 41–45.
[18] J. Humlíček, M. Garriga, M.I. Alonso, M. Cardona, Optical spectra of Si_xGe_{1-x} alloys, J. Appl. Phys. 65 (1989) 2827–2832.
[19] E.D. Palik, Chapter 14 – Optical Parameters for the Materials in HOC I and HOC II, in: Handbook of Optical Constants of Solids, Academic Press, Burlington, 1997, pp. 313–335.
[20] J.A. Woollam, S. Ellipsometers, Smarter Spectroscopy, J.A. Woollam Co., Inc., 2012.
[21] E. Nolot, J.M. Hartmann, J. Hilfiker, Optical constants determination of pseudomorphic $Si_{1-x}Ge_x$ layers on Si(001), with $0 < x < 0.54$, in: D. Harame, M. Caymax, M. Heyns, G. Masini, S. Miyazaki, G. Niu, A. Reznicek, K. Saraswat, B. Tillack, B. Vincent, Y.C. Yeo, A. Ogura, J. Murota (Eds.), Sige, Ge, and Related Compounds 6: Materials, Processing, and Devices, 2014, pp. 455–465.
[22] Devki N. Talwar et al. (unpublished).